Chinese Chemical Letters 35 (2024) 109414

Contents lists available at ScienceDirect

Chinese Chemical Letters

journal homepage: www.elsevier.com/locate/cclet

Tetrahedral framework nucleic acids promote the proliferation and differentiation potential of diabetic bone marrow mesenchymal stem cell

Yanjing Li[a], Jiayin Li[a], Yuqi Chang[a], Yunfeng Lin[b,*], Lei Sui[a,*]

[a] Department of Prosthodontics, Tianjin Medical University School and Hospital of Stomatology, Tianjin 300070, China
[b] State Key Laboratory of Oral Diseases, West China Hospital of Stomatology, Sichuan University, Chengdu 610041, China

ARTICLE INFO

Article history:
Received 28 August 2023
Revised 10 December 2023
Accepted 12 December 2023
Available online 23 December 2023

Keywords:
Bone marrow mesenchymal stem cell
Diabetes mellitus
DNA-based nanomaterial
Tetrahedral framework nucleic acids
Endogenous bone regeneration

ABSTRACT

Diabetes mellitus considerably affects bone marrow mesenchymal stem cells (BMSCs), for example, by inhibiting their proliferation and differentiation potential, which enhances the difficulty in endogenous bone regeneration. Hence, effective strategies for enhancing the functions of BMSCs in diabetes have far-reaching consequences for bone healing and regeneration in diabetes patients. Tetrahedral framework nucleic acids (tFNAs) are nucleic acid nanomaterials that can autonomously enter cells and regulate their behaviors. In this study, we evaluated the effects of tFNAs on BMSCs from diabetic rats. We found that tFNAs could promote the proliferation, migration, and osteogenic differentiation of BMSCs from rats with type 2 diabetes mellitus, and inhibited cell senescence and apoptosis. Furthermore, tFNAs effectively scavenged the accumulated reactive oxygen species and activated the suppressed protein kinase B (Akt) signaling pathway. Overall, we show that tFNAs can recover the proliferation and osteogenic potential of diabetic BMSCs by alleviating oxidative stress and activating Akt signaling. The study provides a strategy for endogenous bone regeneration in diabetes and also paves the way for exploiting DNA-based nanomaterials in regenerative medicine.

Diabetes mellitus, a globally prevalent metabolic disease, is characterized by hyperglycemia and causes a series of complications. Clinical evidence shows notable effects of diabetes mellitus on bone, such as attenuated bone remodeling, aggravated bone loss, increased risk of fractures, and impaired bone healing [1]. Mechanistically, hyperglycemia can induce severe oxidative stress [2,3] or directly alter bone cells [4], ultimately resulting in alterations in the bone. Bone marrow mesenchymal stem cells (BMSCs), the seed cells in bone formation, can be significantly affected by diabetes, which results in inhibition of proliferation and differentiation leading to stem cell exhaustion and reduced bone formation. Considering its deleterious effects on bone, strategies such as BMSCs transplantation have been developed to achieve fast and ideal fracture healing and bone regeneration under diabetes mellitus [5,6]. Transplantation of exogenous BMSCs contributes to direct ossification, however, BMSCs application is limited by immune rejection, infection, tumorigenesis, limited sources, and ethical issues [7,8]. Besides, the proliferation and differentiation potential of BMSCs is largely reduced upon *in vitro* expansion. Therefore, reactivation of impaired BMSCs may promote endogenous bone regeneration in diabetes.

Chronic diabetes leads to unusually high concentrations of reactive oxygen species (ROS) in BMSCs, resulting in severe oxidative stress [9]. The accumulated ROS can directly alter gene expression and signal transduction, which may lead to inhibited proliferation and differentiation potential of BMSCs. ROS are thus proposed to be candidate regulators of BMSCs in diabetes. Small molecules, such as melatonin, morroniside, and 2-cyanopyrrolidine alpha-amino amide can effectively protect BMSCs from oxidative stress and promote their osteogenic ability [10–13]. However, their application is restricted by poor stability, weak endocytic efficiency, and low bioavailability. Singh *et al.* constructed a nanoceria-tailored scaffold to relieve oxidative stress in MSCs under diabetic conditions and recapitulated the cellular microenvironment [14]. This scaffold significantly stimulated the osteogenic differentiation of stem cells and enhanced early bone regeneration in diabetes. Tian *et al.* constructed an electronically modulated metal oxide to protect MSCs from ROS and promote tissue regeneration [15]. Nevertheless, the application of these nanomaterials is limited by complicated synthesis, unknown long-term biocompatibility, and other factors.

* Corresponding authors.
E-mail addresses: yunfenglin@scu.edu.cn (Y. Lin), suilei@tmu.edu.cn (L. Sui).

https://doi.org/10.1016/j.cclet.2023.109414
1001-8417/

In a previous study, we demonstrated that tetrahedral framework nucleic acids (tFNAs), which are nucleic acid nanomaterials, could scavenge ROS and regulate the biology and fate of cells [16]. tFNAs are designed and constructed using four isometric single-stranded DNA molecules through one-pot annealing [17–19]. They possess unique advantages, such as a simple method of synthesis, relatively high yield, excellent editability and modification versatility, outstanding biocompatibility and biodegradability, which may be due to the nature of nucleic acids. Moreover, owing to their unique dimensions and spatial structure, tFNAs can pass through the plasma membrane without the help of transfection reagents. Besides, tFNAs can be loaded with nucleic acid drugs to further exert their therapeutic effects [20–22]. In previous studies, we confirmed that tFNAs can regulate cell behavior, for instance, they can promote the proliferation and migration of adipose-derived stem cells [23,24], and considerably enhance the proliferation and osteogenic differentiation of periodontal ligament stem cells [25]. tFNAs can also scavenge ROS and alleviate oxidative stress, owing to the natural ability of DNA [26,27]. tFNAs protect endothelial cell function and enhance diabetic wound healing *via* impeding oxidative damage [28]. They ameliorate insulin resistance of hepatic cells in diabetic individuals by scavenging ROS [29]. The effects of tFNAs on BMSCs from diabetic individuals have not been evaluated. We hypothesized that tFNAs could alleviate oxidative stress in BMSCs from diabetic individuals and promote their proliferation and differentiation potential. In this study, we evaluated the effects of tFNAs on BMSCs from diabetic rats. This study provides evidence for the potential application of tFNAs and should help devise a strategy for endogenous bone regeneration in diabetes patients.

All animal experiments were approved by the Ethics Committee of Tianjin Medical University. Five-week-old Sprague-Dawley rats were purchased from Department of Laboratory Animal Science, Tianjin Medical University and assigned to the control or type 2 diabetes mellitus (T2DM) group after acclimatization. Normal rats were fed a standard diet for 12 weeks. T2DM rats were fed a high-fat diet (HFD, 60% fat by energy) for 4 weeks and then intraperitoneally injected with streptozotocin (30 mg/kg bw). To ensure the establishment of the T2DM rat model, blood concentration of glucose was detected after 3 and 7 days of injection. T2DM rats were fed HFD for 3 months before sacrifice and the femurs were scanned using micro-CT and subsequently fixed and for hematoxylin and eosin (H&E) and tartrate-resistant acid phosphatase (TRAP) staining. BMSCs were extracted from normal and T2DM rats through whole bone marrow adherent culturing as before [30]. Briefly, the femur and tibia were separated and rinsed with alpha minimal essential medium (α-MEM), supplemented with 10% fetal bovine serum (FBS) and 1% penicillin-streptomycin. The cells were cultured at 37 °C in an atmosphere of 5% CO_2 and the medium was changed every 2 d. tFNAs were synthesized using four ssDNA molecules using "one-pot annealing" as reported previously [31,32]. Sequences of the four ssDNAs are shown in Table S1 (Supporting information). The successful synthesis of tFNAs was verified using high-performance capillary electrophoresis (HPCE) and polyacrylamide gel electrophoresis (PAGE). Dynamic light scattering (DLS) was employed to examine the zeta potential and hydrated size of tFNAs. Transmission electron microscopy (TEM) and atomic force microscopy (AFM) were used to determine the size and shape of tFNAs. Cells were incubated with Cy5-labeled tFNAs for 24 h and collected in phosphate-buffered saline. The internalization of tFNAs inside BMSCs was detected using flow cytometry, as described previously [33]. More detailed methods can be found in Supporting information.

Since diabetes affects bone metabolism and leads to increased bone loss, decrease in bone mineral density, and alterations in BMSCs [34,35]. First, we compared the bone architecture and other parameters between normal and T2DM rats. Micro-CT analysis revealed changes in the long bone of T2DM rats (Fig. 1A). Compared with that in normal rats, the cortical thickness of both middle and distal femur in T2DM rats was decreased, and the trabecular number in spongy bone was reduced. The bone mineral density (BMD), bone volume (BV), percent bone volume (BV/TV), and trabecular number (Tb.N) were significantly reduced in the middle femur of T2DM rats (Fig. 1C), and the BMD, BV, BV/TV, trabecular thickness (Tb.Th), and Tb.N were reduced in the distal femur of these rats, while trabecular separation (Tb.Sp) was increased (Fig. 1D). H&E staining of bone sections revealed reduced trabecular number and broken trabeculae, and TRAP staining showed reduced number of osteoclasts (Fig. 1B). A reasonable explanation for the reduction in the numbers of both osteoblasts and osteoclasts is the low bone turnover rate in diabetes [36]. These results indicate obvious bone loss in T2DM rats.

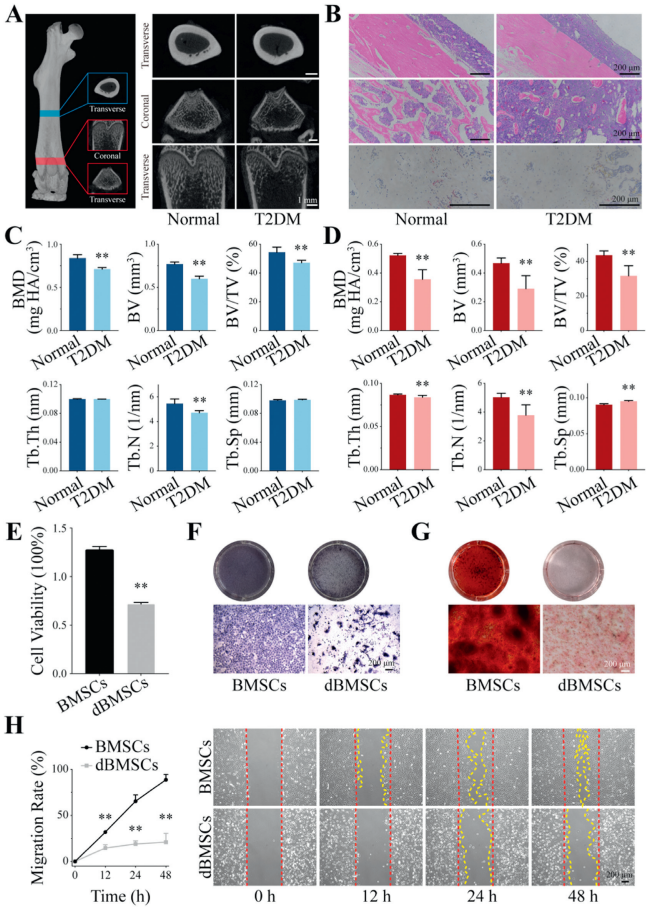

Fig. 1. Characters of diabetic bone and BMSCs. (A) Micro-CT images of the femurs. Scale bar: 1 mm. (B) H&E staining and TRAP staining images. Scale bar: 200 μm. (C) Quantification of morphometric parameters of the middle femoral cortical bone. (D) Quantification of morphometric parameters of the distal femoral trabecular bone. (E) Cell viability of BMSCs. (F) ALP staining images. Scale bar: 200 μm. (G) Alizarin red staining images. Scale bar: 200 μm. (H) Wound healing assay results and the statistical analysis. Scale bar: 200 μm. Data are mean ± standard deviation (SD) ($n = 3$), and are statistically evaluated using the t-test. $^{**}P < 0.01$.

Next, we compared the biological behavior of primary BMSCs obtained from normal and T2DM mice. The results of cell viability analysis showed that the cell viability of diabetic BMSCs was significantly reduced (Fig. 1E). Alkaline phosphatase (ALP) and Alizarin red staining of BMSCs from T2DM rats was weaker than that of BMSCs from normal mice, suggesting reduced osteogenic differentiation (Figs. 1F and G). Cell migration ability was detected using wound-healing assay. BMSCs from T2DM rats exhibited a slower migration rate and lesser closure of the wounds than

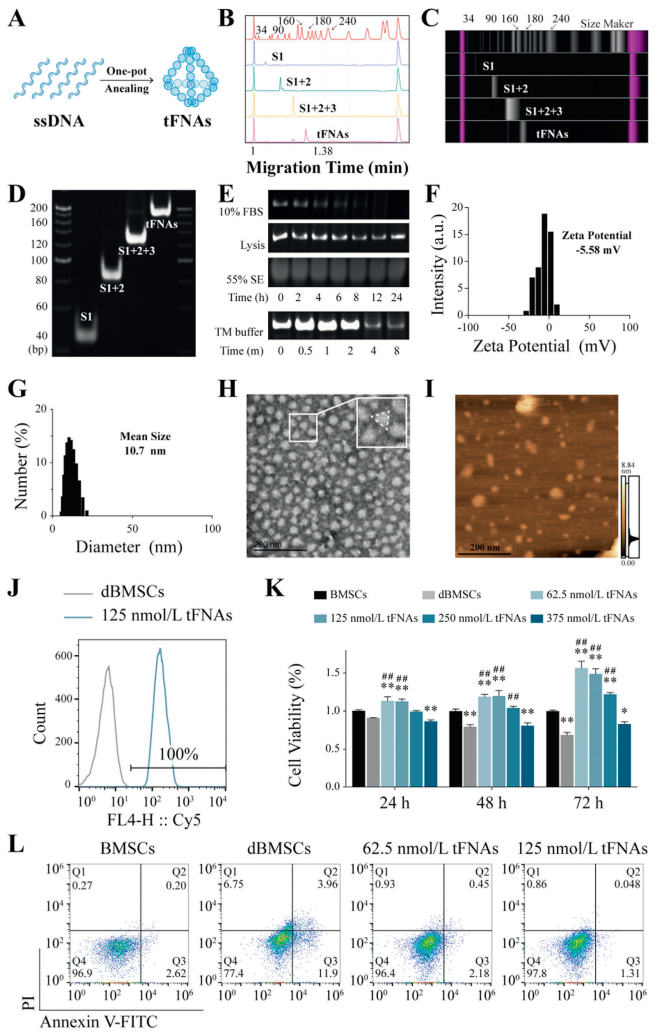

Fig. 2. Fabrication and characteristics of tFNAs. (A) Schematic illustration of the fabrication of tFNAs. (B) HPCE results of tFNAs. (C) Stimulated gel image of HPCE. (D) PAGE results of tFNAs. (E) Stability of tFNAs. (F) Zeta potential of tFNAs. (G) Hydrated size of tFNAs. (H) TEM image of tFNAs. (I) AFM image of tFNAs. Scale bar: 200 μm. (J) Cell uptake of tFNAs. (K) Cell viability of diabetic BMSCs after tFNAs incubation. (L) Cell apoptosis of diabetic BMSCs after tFNAs incubation. Data are mean ± SD ($n = 3$), and are statistically evaluated using the one-way analysis of variance (ANOVA). $^{*}P < 0.05$, $^{**}P < 0.01$ compare with BMSCs. $^{\#\#}P < 0.01$ compare with diabetic BMSCs.

normal BMSCs (Fig. 1H). Thus, BMSCs from T2DM rats displayed changed biological behavior, such as decreased potential for proliferation, osteogenic differentiation, and migration. These changes may lead to reduced quantity and quality of BMSCs, resulting in increased bone loss as well as poor bone turnover rate.

Because we have previously shown that tFNAs promote the proliferation and differentiation of stem cells [31], we speculated that they might play a prominent role in promoting the same in BMSCs from diabetic rats. tFNAs were synthesized as described previous reports from our group [37–39], and the synthesis scheme is shown in Fig. 2A. The successful synthesis of tFNAs was confirmed using HPCE (Figs. 2B and C) and PAGE (Fig. 2D). The molecular weight of tFNAs was determined to be ~174 bp. The stability of tFNAs under physiological environment and storage conditions was determined using PAGE. As is evident from Fig. 2E, tFNAs were stable for about 6 h in 10% FBS, and for 24 h each in cell lysis solution and rat serum. They could be stored for 2 months in storage buffer at 4 °C. The potential of tFNAs was about −5.58 mV (Fig. 2F), and the hydrated size of tFNAs was approximately 10.7 nm (Fig. 2G), which are consistent with our previous results. The diameter of tFNAs determined using TEM (Fig. 2H) and AFM (Fig. 2I) images was approximately 20 nm, and the shape was almost a regular triangle. The above results indicated the successfully fabrication of tFNAs, with properties that were consistent with those reported previously. These tFNAs were used in further experiments.

Next, we incubated primary BMSCs from T2DM rats with tFNAs to assess the effects of the synthesized tFNAs. The uptake of tFNAs by diabetic BMSCs was examined using flow cytometry. tFNAs could completely penetrate the BMSCs from T2DM rats after 24 h of incubation (Fig. 2J); the endocytic efficiency of tFNAs was high probably due to their unique tetrahedral structure and dimension [23,40]. The viability of diabetic BMSCs treated with different concentrations of tFNAs was determined by cell counting kit-8 (CCK-8). The viability of tFNA-treated BMSCs from T2DM rats was higher than that of BMSCs from normal rats and tFNAs significantly promoted the proliferation of the former (Fig. 2K). Flow cytometry analysis showed that tFNAs alleviated the apoptosis of BMSCs from T2DM rats. Compared with BMSCs from normal rats, those from T2DM rats showed much higher cell death, both through apoptosis and necrosis (Fig. 2L); however, tFNA-treated BMSCs from T2DM rats showed less cell death than those from normal rats. These results indicated that tFNAs substantially promoted the proliferation and alleviated the apoptosis BMSCs from T2DM rats, with 125 nmol/L tFNAs showing the maximum effect.

ROS contributes to the malfunctioning of MSCs in diabetes and is associated with diabetic complications. Hence, we examined the ROS levels in BMSCs from diabetic mice. Analyses using a fluorescent probe and flow cytometry showed that BMSCs from T2DM rats had high ROS levels (Figs. 3A and B). When treated with tFNAs, these BMSCs showed lower ROS levels, similar to BMSCs from normal rats. This might be due to the intrinsic ROS-scavenging ability of DNA [26]. Because ROS leads to cell senescence and cell death, we examined the senescence of BMSCs using senescence-associated β-galactosidase staining. As shown in Fig. 3C, almost half of the BMSCs from T2DM rats were senescent, whereas lesser numbers of BMSCs from normal rats and tFNA-treated BMSCs from T2DM rats were stained. Similar results were obtained by quantitative analysis of the staining. These results indicated that tFNAs promote the proliferation and relieve senescence and apoptosis in BMSCs from diabetic rats by alleviating oxidative stress.

Cell migration is important in BMSC-mediated bone regeneration. We, therefore, investigated the migration of BMSCs from T2DM rats after tFNAs treatment. The migration ability of BMSCs from T2DM rats was attenuated after tFNAs treatment (Fig. 3D). The cell mobility of BMSCs from T2DM rats was notably reduced; however, when treated with tFNAs, a non-significant difference in the mobility of these BMSCs compared with that of BMSCs from normal rats was noted. Next, the osteogenic differentiation of BMSCs was evaluated using ALP staining and Alizarin red staining. ALP staining is an indicator of the early osteogenic ability. BMSCs from T2DM rats showed reduced ALP levels whereas tFNAs treatment enhanced the ALP production (Fig. 3E). Alizarin red staining is used to evaluate the mineralized nodes and is an indicator of the late osteogenic ability. The results of Alizarin red staining were consistent with those of ALP staining (Fig. 3F). Moreover, the levels of osteogenic markers were detected by Western blot and qPCR analyses. Runt-related transcription factor 2 (Runx2) is the master transcription factor in osteogenic differentiation of BMSCs, which upregulates the expression of important osteogenic factors, such as ALP, osteopontin (OPN), and osteocalcin (OCN) [41,42]. The expression of Runx2 was reduced in BMSCs from T2DM rats but was restored in BMSCs after tFNAs (Figs. 3G and I). The transcription level of *Alp* and *Opn* were also examined. The mRNA levels of *Alp* and *Opn* in BMSCs from T2DM rats were upregulated after incubation with tFNAs (Fig. 3H). These results indicate that tFNAs can rescue

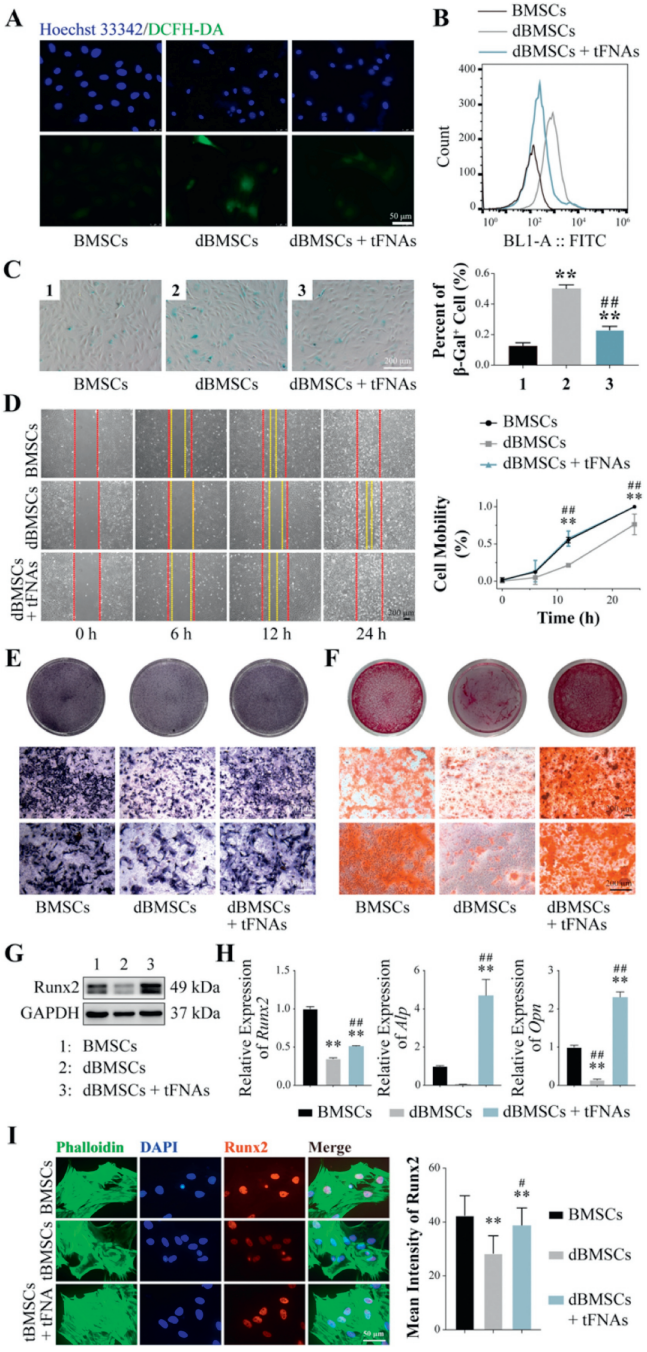

Fig. 3. tFNAs promote the cell behaviors of BMSCs from diabetic rats. (A) ROS generation in diabetic BMSCs detected by DCFH-DA probe. Scale bar: 50 μm. (B) ROS generation detected by flow cytometry. (C) senescence-associated β-galactosidase staining and statistical analysis of diabetic BMSCs after tFNAs incubation. Scale bar: 200 μm. (D) Wound healing assay results and the statistical analysis of diabetic BMSCs after tFNAs incubation. Scale bar: 200 μm. (E) ALP staining results. Scale bar: 200 μm. (F) Alizarin red staining results. Scale bar: 200 μm. (G) Expression of Runx2. (H) Relative expression of *Alp*, *Runx2*, *Opn*. (I) Immunofluorescence staining and quantitative analysis of Runx2. Scale bar: 50 μm. Data are mean ± SD ($n = 3$), and are statistically evaluated using the one-way ANOVA. $^{*}P < 0.05$, $^{**}P < 0.01$ compare with BMSCs; $^{\#}P < 0.05$, $^{\#\#}P < 0.01$ compare with diabetic BMSCs. GAPDH, glyceraldehyde-3-phosphate dehydrogenase.

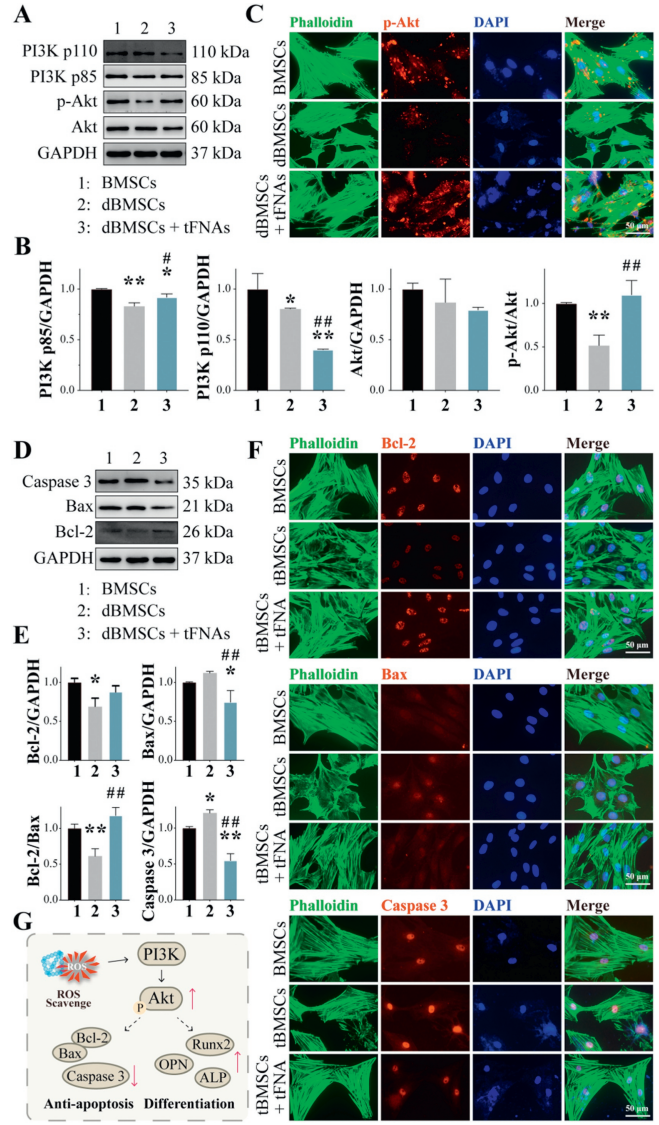

Fig. 4. tFNAs protect diabetic BMSCs *via* PI3K/Akt signaling pathway. (A) Expression of PI3K p85, PI3K p110, p-Akt and Akt. (B) Quantitative analysis of PI3K p85, PI3K p110, and p-Akt. (C) Immunofluorescence staining of p-Akt. Scale bar: 50 μm. (D) Expression of Bcl-2, Bax, and caspase 3. (E) Quantitative analysis of Bcl-2, Bax, and caspase 3. (F) Immunofluorescence staining of Bcl-2, Bax, and caspase 3. Scale bar: 50 μm. (G) Scheme of signaling pathway changes after tFNAs treatment. Data are mean ± SD ($n = 3$), and are statistically evaluated using the one-way ANOVA. $^{*}P < 0.05$, $^{**}P < 0.01$ compare with BMSCs; $^{\#}P < 0.05$, $^{\#\#}P < 0.01$ compare with diabetic BMSCs. DAPI, 4′,6-diamidino-2-phenylindole.

the impaired osteogenic differentiation ability of BMSCs from diabetic rats.

Deeper insights into the mechanisms underlying the biology of BMSCs from diabetic rats revealed that hyperglycemia affects gene expression *via* the phosphatidylinositide 3-kinases/protein kinase B (PI3K/Akt) signaling pathway [43]. Akt is a highly conserved intracellular signal pathway that plays central regulatory roles in the proliferation, survival, migration, differentiation, and senescence of stem cells [44,45]. Akt activation is achieved by phosphorylation and is followed by the activation of downstream proteins and promotion of the functioning of cells. Strategies for activating Akt signaling in stem cells have been intensively researched and used for promoting cell activity and tissue engineering. BMSCs from T2DM mice showed suppression of activated Akt, which is considered to be the reason for decreased cell proliferation and differentiation capability [46]. We determined the levels of PI3K and Akt to explore the mechanism underlying the effects of tFNAs on BMSCs from diabetic rats. The PI3K p85 was reduced in BMSCs from T2DM rats, and was upregulated after tFNAs treatment (Figs. 4A and B). The total Akt level remained constant in BMSCs from normal and diabetic rats, and in BMSCs from diabetic rats incubated

with tFNAs, whereas the levels of phosphorylated Akt (p-Akt) were reduced in BMSCs from T2DM rats, and were upregulated after tFNA treatment. Immunofluorescence analysis showed similar results (Fig. 4C).

The suppressed PI3K/Akt signaling pathway may lead to cell apoptosis through Bcl-2/Bax imbalance and caspase cascade. Here, the level of Bcl-2, Bax, and caspase 3 were examined. As shown in Figs. 4D and E, the expression level of Bcl-2 was reduced in BMSCs from T2DM mice, and rescued in tFNAs treated diabetic BMSCs. Bax was slightly increased in BMSCs from T2DM mice, while decreased in tFNAs treated diabetic BMSCs. The imbalance of Bcl-2/Bax could triggered the caspase cascade, and finally result in cell apoptosis [47]. Caspase 3 was significantly increased in BMSCs from T2DM mice, and the boosted caspase 3 was inhibited after tFNAs incubation. Immunofluorescence analysis showed similar results (Fig. 4F). These results displayed that tFNAs can reserve cell apoptosis through PI3K/Akt signaling pathway in BMSCs from diabetic rats. All the above indicates the mechanism underlying the effects of tFNAs on the proliferation and differentiation potential of BMSCs from diabetic rats (Fig. 4G). tFNAs can scavenge the excess ROS in diabetic BMSCs, and reactivate the suppressed PI3K/Akt signaling pathway, leading to the inhibited caspase 3 and stimulated Runx2, which result in anti-apoptosis and osteogenic differentiation respectively.

In conclusion, BMSCs from T2DM rats exhibited several alterations in their functions, such as decreased proliferation and differentiation capacity, which may lead to increased bone loss and difficulty in bone regeneration. tFNAs could autonomously enter the cells and regulate their behavior. tFNAs promoted the proliferation, migration, and osteogenic differentiation potential of BMSCs from T2DM rats, and alleviated cell senescence and apoptosis. The excellent effects of tFNAs on BMSCs from diabetic rats may be due to the alleviation of oxidative damage and activation of the Akt signaling pathway. The study provides a practical strategy for improving the function of BMSCs and envisages an approach for endogenous bone regeneration in diabetes patients.

Declaration of competing interest

The authors declare that they have no known competing financial interests or personal relationships that could have appeared to influence the work reported in this paper.

Acknowledgments

This study was supported by National Natural Science Foundation of China (No. 82301030), China Postdoctoral Science Foundation (No. 2022M712384), Tianjin Education Commission Research Project (No. 2021KJ244), and Tianjin Health Science and Technology Project (No. TJWJ2021QN038), and Tianjin Key Medical Discipline (Specialty) Construction Project (No. TJYXZDXK-038A).

Supplementary materials

Supplementary material associated with this article can be found, in the online version, at doi:10.1016/j.cclet.2023.109414.

References

[1] L.C. Hofbauer, B. Busse, R. Eastell, et al., Lancet Diabetes Endocrinol. 10 (2022) 207–220.
[2] L.S. Tan, J.T. Chen, L.Y. Lim, et al., Cell Prolif. 55 (2022) e13232.
[3] N. Jiang, H. Zhao, Y.C. Han, et al., Cell Prolif. 53 (2020) e12909.
[4] F. Giacco, M. Brownlee, Circ. Res. 107 (2010) 1058–1070.
[5] K. Al-Hezaimi, S. Ramalingam, M. Al-Askar, et al., Int. J. Oral Sci. 8 (2016) 7–15.
[6] M.J. Devine, C.M. Mierisch, E. Jang, et al., J. Orthop. Res. 20 (2002) 1232–1239.
[7] T. Ouchi, T. Nakagawa, Regen. Ther. 14 (2020) 72–78.
[8] J. Gao, C. Gao, Cell Prolif. 55 (2022) e13217.
[9] C.L. Bigarella, R. Liang, S. Ghaffari, Development 141 (2014) 4206–4218.
[10] F. Munmun, P.A. Witt-Enderby, J. Pineal Res. 71 (2021) e12749.
[11] Y. Sun, Y. Zhu, X. Liu, et al., Cell Prolif. 53 (2020) e12866.
[12] P.C. Tang, Z.G. Lin, Y. Wang, et al., Chin. Chem. Lett. 21 (2010) 253–256.
[13] P.F. Xiao, R. Guo, S.Q. Huang, et al., Chin. Chem. Lett. 25 (2014) 673–676.
[14] R.K. Singh, D.S. Yoon, N. Mandakhbayar, et al., Biomaterials 288 (2022) 121732.
[15] Q. Tian, W. Wang, L. Cao, et al., Adv. Mater. 34 (2022) e2207275.
[16] T. Tian, T. Zhang, S. Shi, et al., Nat. Protoc. 18 (2023) 1028–1055.
[17] R.P. Goodman, I.A.T. Schaap, C.F. Tardin, et al., Science 310 (2005) 1661–1665.
[18] S.R. Shi, T.Y. Chen, W.T. Lu, et al., Adv. Funct. Mater. (2023) 2305558.
[19] T. Zhang, H.S. Ma, X.L. Zhang, et al., Adv. Funct. Mater. 33 (2023) 2213401.
[20] L.M. Zhang, L.F. Xu, Y. Wang, et al., Chin. Chem. Lett. 33 (2022) 4089–4095.
[21] Z.K. Guo, B.J. Jin, Y.L. Fang, et al., Chin. Chem. Lett. 33 (2022) 4208–4212.
[22] M. Liu, L. Hao, D. Zhao, et al., ACS Appl. Mater. Interfaces 14 (2022) 38506–38514.
[23] S. Shi, Y. Li, T. Zhang, et al., ACS Appl. Mater. Interfaces 13 (2021) 57067–57074.
[24] T.Y. Chen, D.X. Xiao, Y.J. Li, et al., Chin. Chem. Lett. 33 (2022) 2517–2521.
[25] M. Zhou, N. Liu, Q. Zhang, et al., Cell Prolif. 52 (2019) e12566.
[26] T. Zhang, T. Tian, Y. Lin, Adv. Mater. 34 (2022) e2107820.
[27] T. Tian, Y. Li, Y. Lin, Bone Res. 10 (2022) 40.
[28] S. Lin, Q. Zhang, S. Li, et al., ACS Appl. Mater. Interfaces 12 (2020) 11397–11408.
[29] Y. Li, Y. Tang, S. Shi, et al., ACS Appl. Mater. Interfaces 13 (2021) 40354–40364.
[30] H. Peng, M. Yang, Q. Guo, et al., Cell Prolif. 52 (2019) e12624.
[31] S. Li, T. Tian, Z. Tao, et al., Mater. Today 24 (2018) 57–68.
[32] Y. Li, S. Gao, S. Shi, et al., Nano-Micro Lett. 13 (2021) 86.
[33] S. Shi, J. Xie, J. Zhong, et al., Cell Prolif. 49 (2016) 341–351.
[34] B. Lecka-Czernik, Diabetologia 60 (2017) 1163–1169.
[35] C.E. Murray, C.M. Coleman, Int. J. Mol. Sci. 20 (2019) 4873.
[36] R.T. Turner, S.P. Kalra, C.P. Wong, et al., J. Bone Miner. Res. 28 (2013) 22–34.
[37] T. Zhang, T. Tian, R. Zhou, et al., Nat. Protoc. 15 (2020) 2728–2757.
[38] Y. Xie, J.J. He, S.H. Li, et al., Adv. Funct. Mater. 33 (2023) 2303580.
[39] R. Yan, W. Cui, W. Ma, et al., ACS Nano 17 (2023) 8767–8781.
[40] L. Liang, J. Li, Q. Li, et al., Angew. Chem. Int. Ed. 53 (2014) 7745–7750.
[41] W.C.W. Chan, Z. Tan, M.K.T. To, et al., Int. J. Mol. Sci. 22 (2021) 5445.
[42] L. Zheng, Q. Tu, S. Meng, et al., J. Cell. Physiol. 232 (2017) 182–191.
[43] J.M. Ryu, M.Y. Lee, S.P. Yun, et al., J. Cell. Physiol. 224 (2010) 59–70.
[44] P. Dentelli, C. Barale, G. Togliatto, et al., Diabetologia 56 (2013) 173–184.
[45] J. Chen, R. Crawford, C. Chen, et al., Tissue Eng. Part B: Rev. 19 (2013) 516–528.
[46] M. Mahmoud, N. Abu-Shahba, O. Azmy, et al., Stem Cell Rev. Rep. 15 (2019) 194–217.
[47] A. Ashkenazi, W.J. Fairbrother, J.D. Leverson, et al., Nat. Rev. Drug Discov. 16 (2017) 273–284.